A FIELD-SPLICED PRESTRESSED JOINT TO EXTEND SPANS OF SIMPLY SUPPORTED I-GIRDERS

Natassia R. Brenkus, ME, Dept. of Civil Engineering, University of Florida, Gainesville, FL
Trey Hamilton, PE, PhD, Dept. of Civil Engineering, University of Florida, Gainesville, FL

ABSTRACT

This paper describes the design and flexural testing of a joint design for a spliced prestressed precast I-girder, for its intended use as a "field-spliced" moment-carrying connection in a 210+ ft simply-supported bridge span – to achieve span lengths beyond current transportation limits for precast segments. The design intends for the joint area to be prestressed at the job-site, utilizing hydraulic jacks mounted to the girder web face to push apart coupled precast segments. The developed splicing method considers current construction practices and the steps of the method are presented. Flexural static testing of the spliced beam specimens is described and the spliced beams' behavior is compared with typical prestressed beam design. The final product was a repeatable cast-in-place prestressed splice design and construction technique to achieve longer spans with prestressed precast members.

Keywords: Prestressed, Precast, Bridge, Splice, Coupler, I-girder

INTRODUCTION

Due to current transportation limitations, precast prestressed concrete girders are limited to transportable spans of approximately 160 ft[1]. Design situations exist, however , for which a simply-supported long-span girder longer than this limit would be beneficial; in limited access construction sites, for example, or where environmental impact must be limited, a longer simple span would be ideal[2].

This paper describes the design and laboratory construction of a splice connection and construction technique to extend simply-supported prestressed concrete I-girder spans. A comparison of the tested flexural capacities of the test specimens is compared with code-predicted values.

LITERATURE REVIEW

Several types of concrete girder splices are currently in use in highway bridge construction, including nonprestressed splices, stitched splices and post-tensioned splices. The most common type is the cast-in-place splice. Whereas the cast-in-place splice is not the most economical, it is the most popular due to its simple construction and flexibility with regards to field tolerances.

One significant benefit of spliced long-span precast concrete girders is their ability to accommodate curved alignments. When a curve in the roadway is required, the splice location can be situated in order to provide a point of curvature between short segment lengths[3]. Similarly, spliced segments can be arranged such that the placement of the piers avoids obstacles on the ground, such as railroad tracks, utilities or other roadways[2]. Because the designer has more flexibility when specifying span lengths and locations of piers, spliced construction allows the placement of piers and spans as necessary for the geometry of the road[4,3].

The utilization of precast concrete (PCC) spliced girders for long spans offers multiple advantages over steel, including increased durability, rapid erection, condensed overall construction time, limited or no environmental impact, reduced cost, and simplified transportation of construction materials[3,5]. Furthermore, steel sections require extensive maintenance and present potential environmental risk when being stripped and repainted; again, the use of spliced concrete bridge girders appears to be an attractive alternative. In environmentally sensitive areas, such as Rock Cut Bridge in Washington, spliced PCC girders provide an ideal solution for eliminating risk to river wildlife[6].

A construction technique for splicing together two precast prestressed girders was presented by Gerwick[7] . In this approach, precast segments are prestressed in the same prestressing bed and a gap is left at midspan during casting (Figure 1). The units are folded about the midspan and transported side-by-side to the site. The segments are then placed on falsework in the final configuration and jacked apart in the splice region to stress the prestressing strands. With the jacks in place, the splice concrete is cast. After curing, the jacks are removed, leaving the splice concrete in a prestressed state.

Disadvantages of this method are the need to predetermine the gap length and to transport all segments on the same truck. As a part of this research, a modified splice technique was developed to allow separate casting of the precast segments.

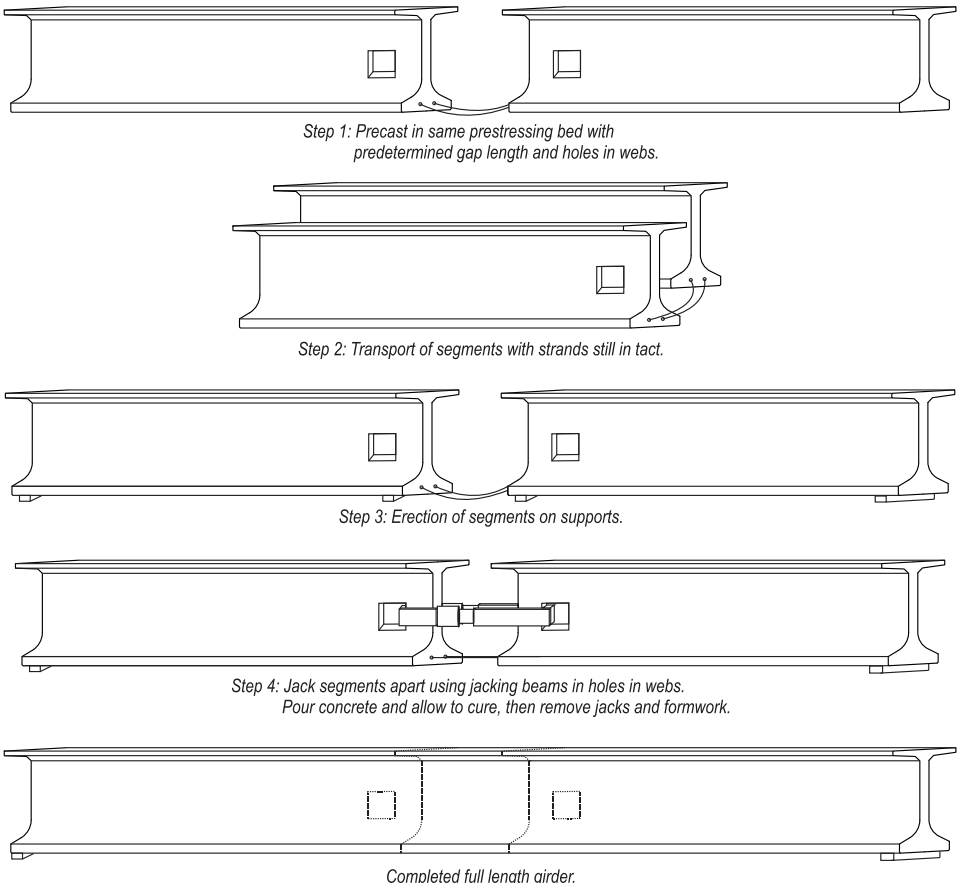

Figure 1 - Prestressing against internal restraint (after Gerwick 1993)

DESIGN CONCEPT

The goal of the project was to develop a method to splice precast prestressed girders while introducing prestress force to the cast-in-place closure pour. The intended application was to extend span lengths of simply-supported prismatic I-girders. Several design requirements guided the design:

- Precompression of the splice region
- A target prestress level of $0.6f_{pu}$
- I-girder cross-section (no end-blocks)
- Prestress force to be imparted without the use of post-tensioning

With these limitations in mind, a variation of the concept presented by Gerwick[7] was developed. As illustrated in Figure 2, Gerwick's proposed splice method was modified for the prototype design such that the strands are cut prior to transport and then spliced on site.

Separation of the precast segments allows for easier precasting, transportation and on-site adjustment during erection. Prestressing force is applied to the system by a hydraulic jack on each side of the girder web. External brackets transfer the force from the hydraulic jacks to the precast segments by thru-bolts that pass through the web of the beam. The internal restraint provided by the coupled prestressing strand resists the jacking force, and the prestressing strand is stressed. The eccentricity between the applied jacking force and the resisting strand creates a lifting moment that is resisted by the self-weight of the precast segments and external tie-downs. After the target stress is achieved, the hydraulic jacks are locked and the splice concrete is placed.

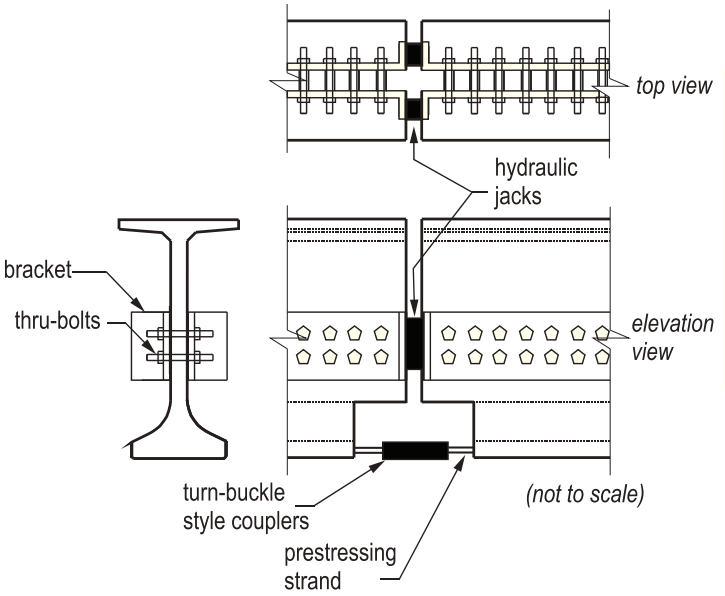

Figure 2–Prototype splice design

PROTOTYPE APPLICATION

A theoretical simple-span bridge was designed as the intended application for the splice connection. Capable of spanning 208 ft, the longest-spanning Florida I-beam, the FIB96, was selected as the cross-section of interest (Figure 3(a)). The exterior girder of the bridge shown in Figure 3(b) was designed using the FIB96 in accordance with AASHTO-LRFD 2007 and the FDOT Structural Design Guidelines[8,9].

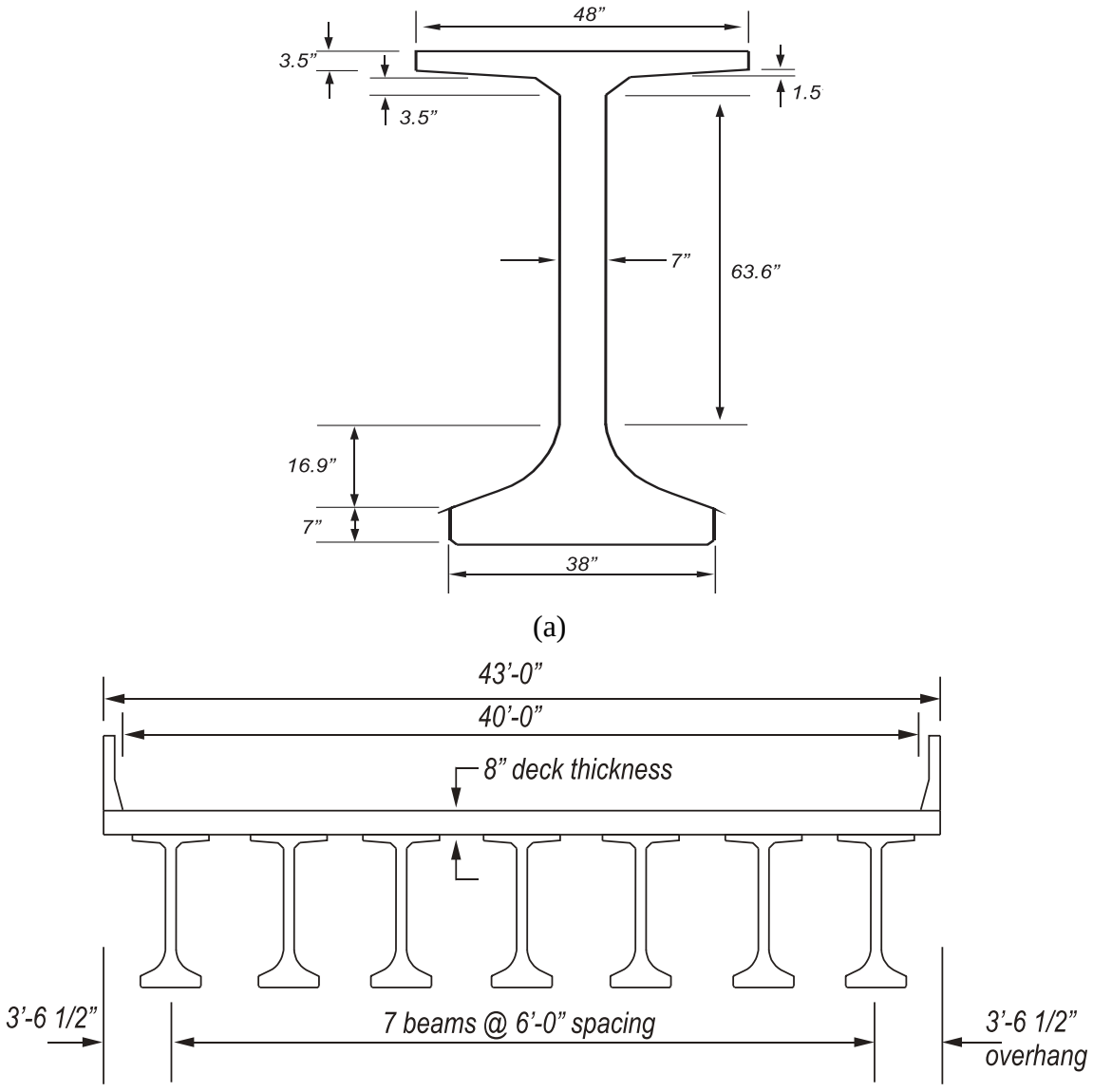

Figure 3 – Prototype design (a) FIB96 and (b) bridge cross-section

Splice locations were selected to occur away from the maximum moment, symmetrically about midspan such that each precast segment was of transportable length. Using the shear and moment demand from the FIB96 prototype design, a strand pattern was determined for the selected splice locations. Assumed splice locations are shown in Figure 4. The strand pattern is shown in Figure 5. For additional information on the FIB96 prototype design, see the FDOT report[10].

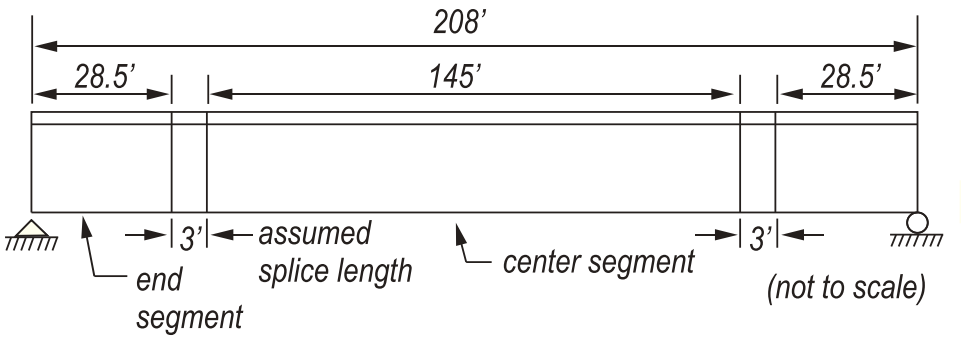

Figure 4 – Elevation view of FIB96 with two splices

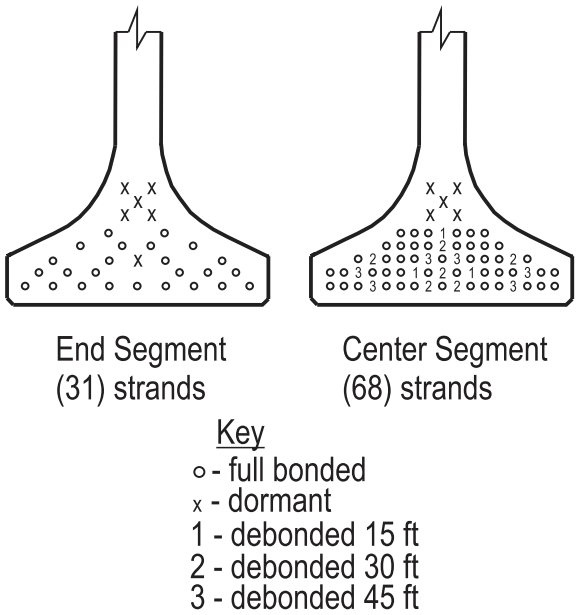

Figure 5 – Strand layouts

SPLICE AND SPECIMEN DESIGN

With the number of strands identified, the splice connection design for the prototype application was developed. The splice design was a modification of a prestress application technique described by Gerwick[7]. The main components of the design included:

- Continuity of prestressing strand across the splice length achieved by turn-buckle style strand couplers.
- Couplers located at the same location along the span length; the strand pattern adjusted to provide clearance.
- Prestress force applied via removable hydraulic jacks.
- The prestress force imparted to the precast segments via steel brackets attached to the precast web with through-bolts.

- Debond the tendon for a short length adjacent to the splice to ensure prestress force on splice is not lost. Subsequent testing also indicated that this provided ductility to the splice.

Due to the large size of the FIB96, the prototype splice design could not be tested in a laboratory setting. To assess the feasibility and repeatability of the splice design and technique, a test specimen was designed to investigate key behavior and constructability concerns.

The chosen test specimen was an AASHTO Type II, selected based on laboratory capabilities. The strand quantity for the test specimen was determined by moment-curvature analysis. Matching the strain in the bottom row strand of the prototype to that of the test specimen at ultimate, a strand quantity was determined for the test specimen. A representation of the strain matching is shown in Figure 6.

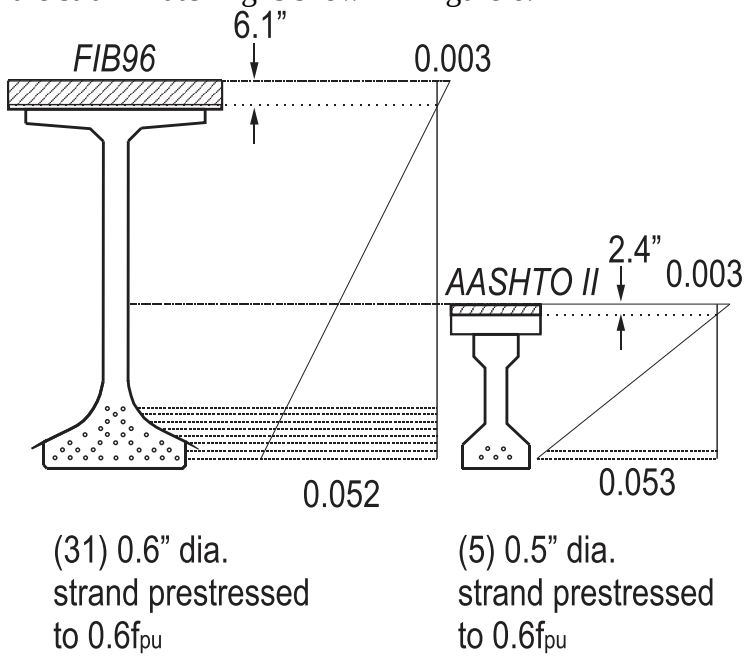

Figure 6 – FIB96 prototype vs. AASHTO II test specimen: strain at flexural capacity

The locations of the five strands in the test specimen were chosen to recreate some of the hardware congestion of the couplers in the FIB96 prototype. The bonding pattern of the test specimen was chosen to mimic the bonding pattern in the prototype near the splice location: an unbonded length of strand was included in the test specimen to provide a longer gage length to reduce prestress losses during stressing. For additional information on the test specimen rationalization, see the FDOT report[10].

Figure 7 shows the test specimen; Figure 8 shows the strand and bonding pattern. The materials chosen for the test beam design were as follows:

Precast beams: Dimensions and strand pattern (Figure 7): AASHTO Type II
Concrete strength at transfer, $f`_{ci}$ = 6 ksi
Concrete strength at 28 days, f'_c = 8.5 ksi

E_{ci} = 4,012 ksi (AASHTO-LRFD)
E_c = 4,776 ksi (AASHTO-LRFD)
Concrete unit weight, w_c = 150 pcf
Beam length = 25.0 ft

Cast-in-place slab: Slab thickness = 8 in.
Concrete strength at 28 days = 4.5 ksi

Prestressing strands: 1/2 in. dia., seven wire lo-lax strand
Area, per strand = 0.153 $in.^2$
Ultimate strength, f_{pu} = 270 ksi
Prestressing strand modulus of elasticity = 28,500 ksi
Prestress level at jacking = $0.6f_{pu}$

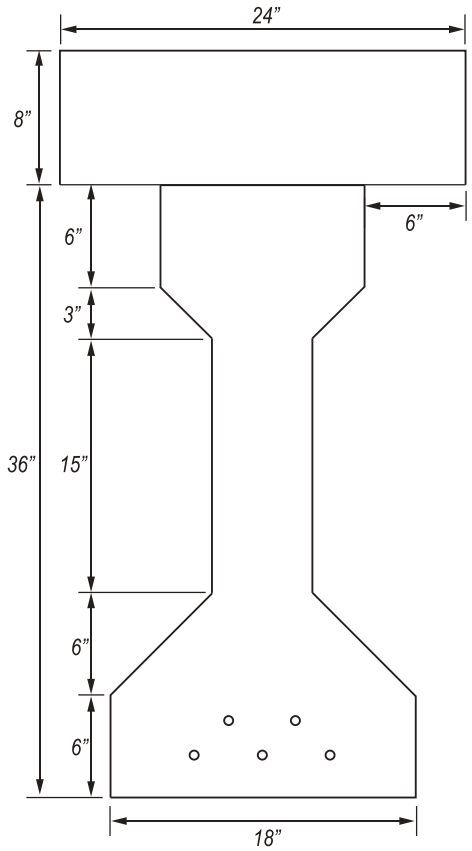

Figure 7 – AASHTO II specimen cross-section

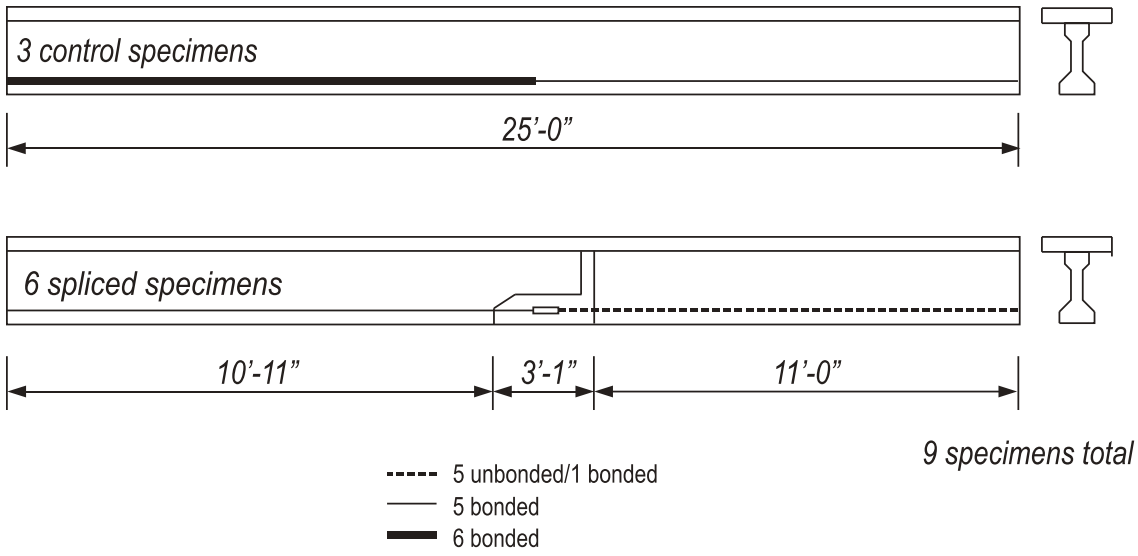

Figure 8 – Test specimens

SPECIMEN CONSTRUCTION AND SPLICE ASSEMBLY

This section describes the splicing procedure as conducted at the Florida Department of Transportation Structures Research Lab.

Three beams 25-ft long were constructed as control beams (specimens XC, FC and SC). Six segments with bonded prestressing 13.5 ft long and six segments with PVC pipes (in future strand locations) 11-ft long were also constructed, to be spliced together at the laboratory to form a 25-ft long completed beam.

Throughout the development of the splice for the FIB96 prototype, the ease of the precast segment construction and the splice assembly procedure was considered, guiding details such as the selection of the type of coupler and the determination of the strand pattern. Assembly of the splice in the AASHTO II test specimen in the laboratory provided an opportunity to evaluate and adjust the procedure. Discrepancies in the precast beam segment geometry, segment alignment, and instrumentation issues aside, the following procedure was followed for each of the six splice assemblies. Table 1 lists the control and spliced specimens (the labels correspond to later load testing). The general set-up of the splice assembly is shown in Figure 9.

Table 1–Specimens

Specimen	Load Test ID	Load Test*
Control	SC	**S**hear
Control	XC	Fle**X**ure
Control	FC	**F**atigue
Spliced 1	X1	Fle**X**ure
Spliced 2	SB	Shear –**B**onded strand in shear span
Spliced 3	SU1	Shear – **U**nbonded

		strand in shear span
Spliced 4	SU2	Shear – **U**nbonded strand in shear span
Spliced 5	F1	**F**atigue
Spliced 6	F2	**F**atigue

*for load test results and discussion, see Brenkus and Hamilton (2013)

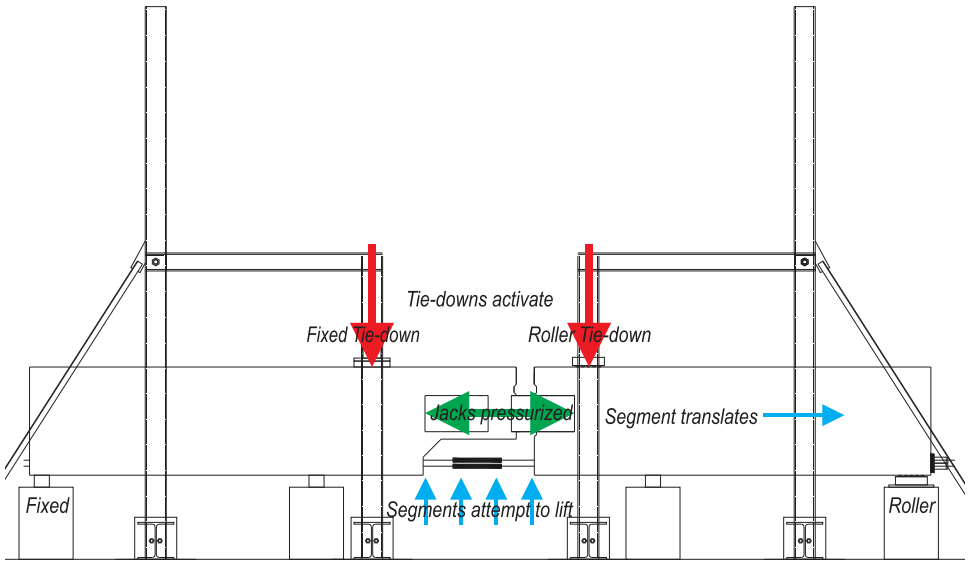

Figure 9 – Elevation: beam segments in frames

Segments were maneuvered into position within the assembly frames and placed on their respective supports. The bonded segment was supported at both ends by wood blocks. One end of the unbonded segment was supported by a wood block; the other end was supported by a Hilman roller welded to a steel block.

The beam segments were then aligned within the frames and longitudinally with one another, ensuring a 5-in. gap between the two segments at the top of the closure gap. Segment heights were adjusted by leveling the bottom of both segments relatively, with particular attention given to the height of the strands. The height of the prestressing strand was used as the controlling point of reference because segment dimensions varied slightly due to construction tolerances; aligning the centroid of the strand provided non-eccentric line of action for the induced prestressing force. Once the beam segments were aligned, wooden cribbing lining the tie-down frames was adjusted to allow unrestrained longitudinal movement of the beam segments along the beam's main longitudinal axis (same direction as the beam span).

Single-acting hydraulic jacks with a mechanical locking ring and hand pumps were set into the brackets on both faces of the beams. The couplers were first installed on the strand protruding from the bonded segment. Engagement of the coupler wedges was checked by attempting to pull each coupler off the strand. The coupler was then installed on the unbonded strand protruding from the unbonded segment.

Next, the hardware (load cells and reusable chucks) at the end of the unbonded segment was loosely installed and the prestressing jacks were simultaneously pressurized until touching both brackets. The lock-nuts were tightened and the hydraulic pressure was released from the jacks. This was done to prevent translation of the unbonded beam segment on the Hilman roller during initial adjustment of the turnbuckle couplers. The hardware for the chucked end of the unbonded segment was then installed (Figure 11).

Figure 10 – Extend plunger of hydraulic jack

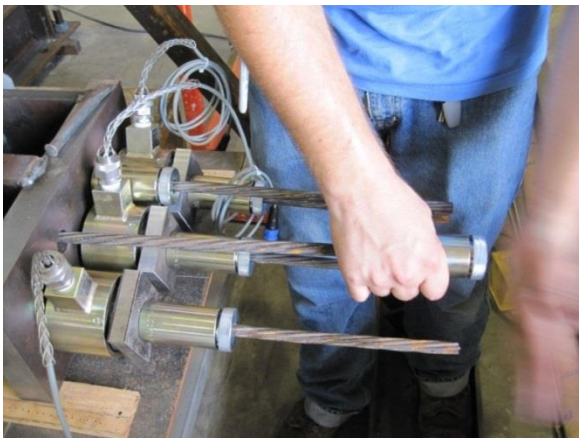

Figure 11 – Chucks and load cells at unbonded segment end

The prestressing strand was then tightened to seat the wedges at the free end of the unbonded segment. With all wedges seated on the strand, an initial load was applied to each strand to straighten the prestressing strand across the closure gap. One person adjusted the turnbuckles on each coupler, another person monitored the alignment of the free end of the unbonded length, making sure that the protruding strand passed clear through the liftoff chair and the load cells without obstruction, and a third person monitored the load cell and coupler strain gage readings (without recording data). Alignment of the load cells was also monitored to ensure that they were flush between the liftoff chair and the prestressing chucks. Approximately 1 kip of load was achieved in each strand, or approximately 100 microstrain per coupler.

Figure 12 – Turnbuckle tightening

Preload in each of the load cells was noted, as well as initial strain in the coupler strain gages. A zero gage reading was taken and the prestressing procedure was started.

Two people were required to operate the hand pumps, while a third monitored the data acquisition system. The prestressing jacks were pressurized synchronously; hand pump operation was synchronized to ensure that the jacks were pressurized equally. Jack pressure was held at 100 psi, then every 500 psi until 5600 psi, corresponding to approximately 25 kip per prestressing strand.

At 5600 psi, the lock-nuts on both jacks were tightened snug by hand. In cases during which 1 in. of longitudinal opening of the gap occurred prior to achieving 5600 psi in the prestressing jacks, the procedure was halted and the lock-nuts were tightened. In the cases where the gap opening between the segments and the load cell readings were both low, jacking was continued until the jack pressure reached 6100 psi. The hydraulic pressure was then simultaneously and slowly released from the jacks. The prestressing strand across the closure pour was—at this point—stressed to approximately $0.6f_{pu}$.

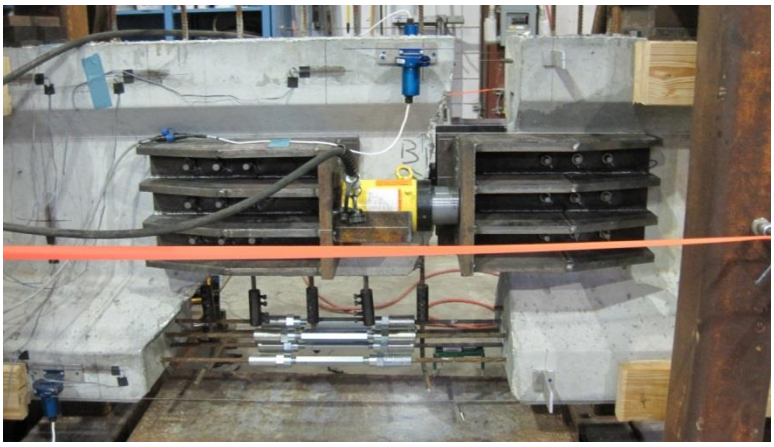

Figure 13 – Splice stressed with lock-nuts engaged

The concrete mix used for the closure pour was a self-consolidating high-strength concrete (SCC) with an f'_c of 8500 psi. An SCC mix was chosen to ensure that the concrete would flow into and completely fill the reentrant corner of the splice.

The concrete was lifted using buckets and funneled into the closure with the aid of a plastic cone. The cone was wedged deeply into the form at the start of the pour, and as the concrete level rose, was slowly extracted in an effort to mitigate segregation of the mix and void formation. A hand-held vibrator was used to vibrate the accessible parts of the pour; however, limited vibration of the closure concrete was possible due to hardware congestion and the placement of instrumentation.

The concrete was allowed to cure until the tested compressive strength – as determined by ASTM C39 tests of 6×12 cylinders made from concrete from the same delivery – reached approximately 8500 psi. This limit was chosen to ensure that the concrete developed some tensile strength prior to removal of the prestressing jacks (during which a small amount of tension is introduced into the joint). The formwork was then removed from the splice region (Figure 14).

Figure 14 – Formwork removed (specimen X1)

To remove the prestressing jacks, they were pressurized until the lock-nuts could be loosened using a spanner wrench. In each case, the pressure required to break the lock-nuts loose was approximately equal to the pressure when the lock-nuts were tightened. This re-pressurization of the jacks was performed simultaneously and slowly, while monitoring the

strand load cells, to prevent over-jacking which would create tensile stress in the fresh concrete and potentially crack the pour. In most cases, the lock-nuts on each actuator broke loose within a few hundred psi of one another and within a few hundred psi of the locked-in pressure.

Next, the tie-down forces were released. A third jack was placed under the beam as near to one end as possible. The interior supports (wood blocks) were knocked out of place to reduce beam restraint. The jack was pressurized until the wood block at this end could be swapped out with a shorter support. The jack pressure was released, replacing the beam on the now lower support, freeing the beam from the tie-down forces at both frames and allowing the completed beam to rest simply-supported.

The brackets were removed and the beam was removed from the assembly frames, completing the splice procedure. Figure 15 shows the completed splice.

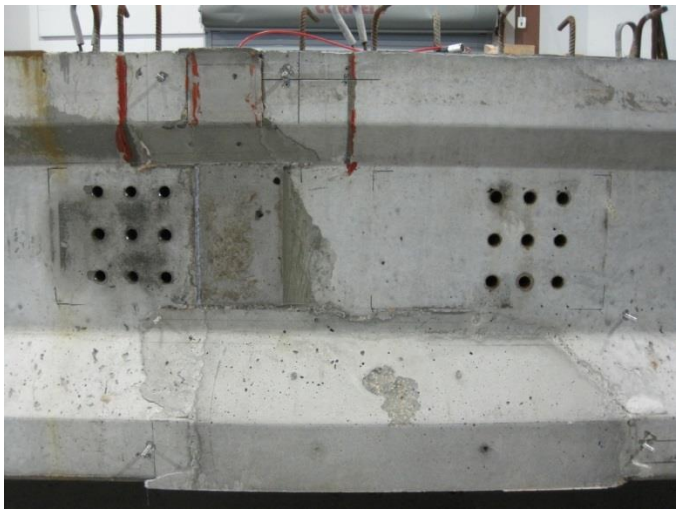

Figure 15 – Splice complete

PRESTRESS AND COMPARISON TO PCI

The goal of the project was to develop a prestressed splice design with a target jacking prestress of $0.6f_{pu}$. This section presents the prestress forces measured in the spliced test specimens during the splicing procedure and compares the effective prestress at different life stages to that expected of a typically prestressed beam and that predicted by typical estimation methods.

Data acquired during the stressing procedure included measurements of:

- three strand load cells on bottom row of strands, measuring strand force
- five calibrated strain gages on each of the couplers, providing an alternate measure of strand force
- four string-pots measuring longitudinal opening of the beam gap
- a single vibrating wire strain gage (VWSG), measuring prestress losses

Figure 16 shows the average strand force versus time for the splice assembly procedure of specimen X1. Also included are the jack pressures at each pause in jacking. The behavior illustrated in the plot is typical of the splice assemblies.

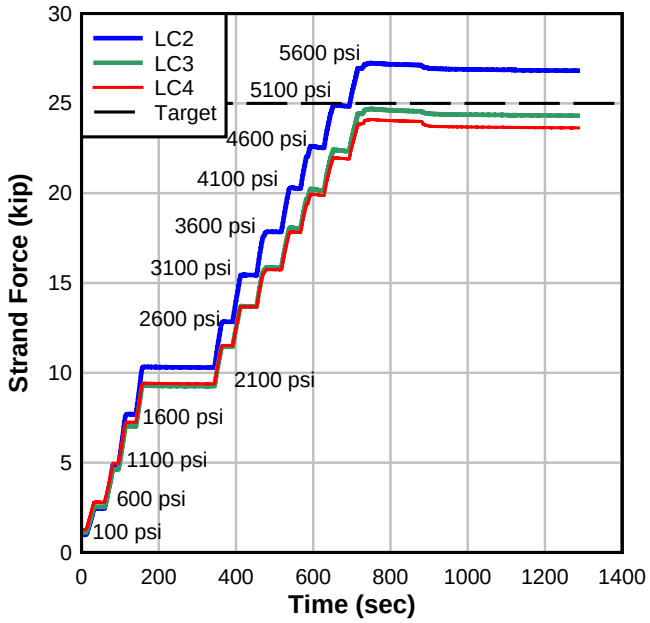

Figure 16 - Load History of X1

Prestress losses were measured with the use of VWSGs; gage locations are shown in Figure 17. The spliced specimens contained two VWSGs – one in the bonded precast segment and one in the middle of the closure pour; for the discussion of prestress losses, only the VWSGs located within the closure pour of each spliced specimen are discussed. The control specimens contained a VWSG in the corresponding location; these gages were used to compute the effective prestress force for each control specimen.

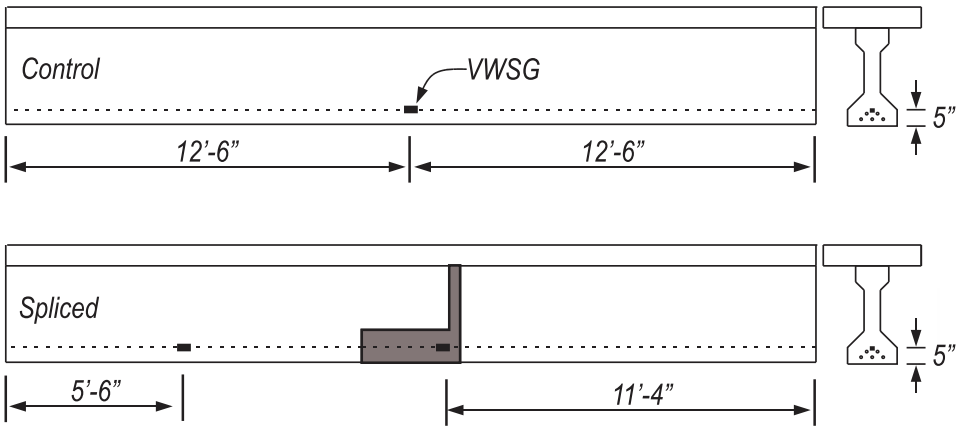

Figure 17 - Placement of VWSG

Figure 18 shows the prestress in each specimen for both the precast control specimens and the spliced specimens versus the age of the concrete. For the VWSG in the precast concrete, a jacking prestress level of $0.6f_{pu}$ was assumed; this jacking prestress was verified with the precast yard's stressing records. To determine the jacking prestress of the splice region of the spliced specimens, the average value of the strand force measured by the three strand load cells was assumed to act at each strand. The x-axis represents the age of the concrete in which the VWSG is encased; this is either the precast concrete or the closure pour for the control and spliced specimens, respectively.

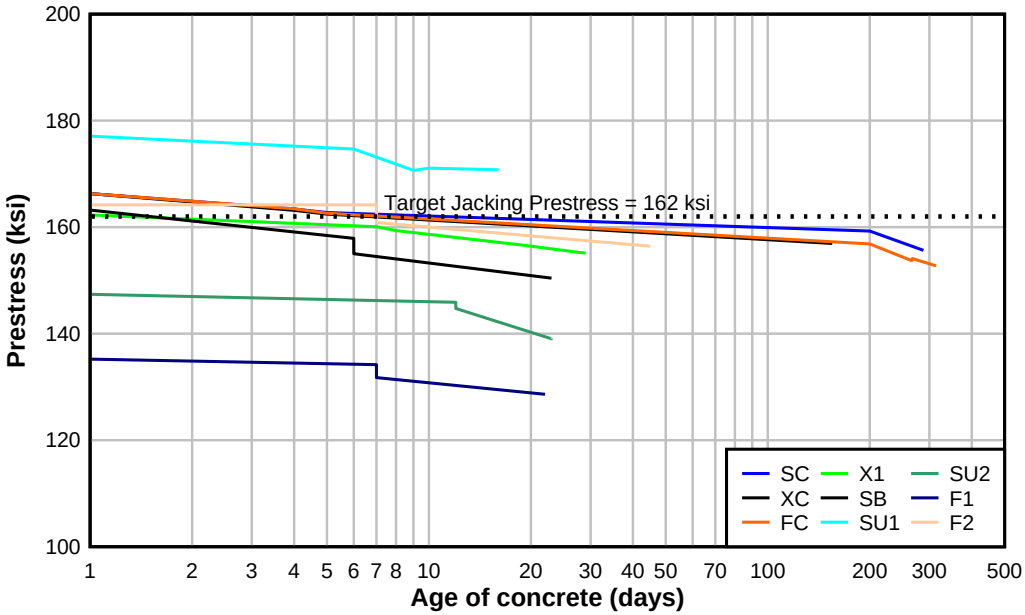

Figure 18 - Prestress force

The control specimens exhibit similar prestress losses. All three control specimens are assumed to have the same prestress at jacking: 166.3 ksi. At prestress transfer (day 4), all three control specimens experience an elastic loss of approximately 3 ksi. Between transfer and the load tests, the three specimens exhibit similar long-term losses, as demonstrated by the similarity of the line slope.

The spliced specimens exhibited two interesting behaviors: prestress loss prior to introduction of the prestress force in the closure pour (which occurred at release of the tie-downs), and decreasing elastic losses with concrete age. For each spliced specimen, the prestress force was introduced into the closure pour approximately 6-7 days after the pour was completed (except for specimen SU2, which was prestressed at day 12). During this time period (prior to prestress of the closure pour), the jacking load was locked off and held in the actuators, resisted by the anchorage at the free end of the unbonded segment. .Prior to prestress of the closure pour, some prestress was lost to creep. Additionally, the effect of the concrete age at the time of the closure pour prestressing is evident: the younger concrete has higher elastic losses. Following this trend, specimen SU2 – with the longest cure prior to release - had the least elastic loss of the spliced specimens.

The VWSG mounted at the centroid of the spliced prestressing strands was used to determine the prestress losses up to load testing. For the precast control specimens, the

jacking force was determined from the calibrated monostrand jack used to stress each strand, as recorded in the stressing records from the precaster. For the spliced specimens, the jacking force is considered to be the prestress force present at tightening of the lock-nut. This prestress force is calculated as the average measurement of the load cells instrumenting the three bottom strands acting in all five strands. The prestress forces at jacking are presented in Table 2.

Table 2-Jacking prestress

Specimen	Average Total Force by Load Cell (kip)	Average Strand Stress (ksi)
SC	127.2	166.3
XC	127.2	166.3
FC	127.2	166.3
X1	124.2	162.3
SB	123.1	161.0
SU1	135.5	177.1
SU2	112.8	147.4
F1	105.7	138.2
F2	125.6	164.1

The initial prestress force is considered the jacking prestress force minus the elastic losses. For all specimens, it was calculated based on prestress losses measured by the VWSGs at the time of prestress transfer, based on the differential strain readings from the VWSG and the Young's modulus of the strand. For the precast control specimens, prestress transfer occurred when the strands were cut free from the bed. For the spliced specimens, the initial force is considered to be the prestress force present just after release of the tie-downs, when the prestress force was imparted to the splice region, causing an immediate elastic loss in the closure pour. Elastic losses between the jacking and the prestress transfer are then revealed.

The effective prestress for all specimens was calculated as the force present at the time of the load test (for the fatigue specimens, the time of the first load test was used) based on the differential strain readings from the VWSG and the Young's modulus of the strand. Long-term losses, such as due to creep and shrinkage, between the jacking and the time of the load test are then revealed. Table 3 shows both the initial and effective prestress force for each completed specimen.

Table 3 – Measured initial prestress

Specimen	Initial prestress		Effective prestress	
	Average Total Force by VWSG (kip)	Average Strand Stress (ksi)	Average Total Force by VWSG (kip)	Average Strand Stress (ksi)
SC	125.0	163.4	119.0	155.6
XC	124.8	163.2	120.1	156.9
FC	125.0	163.4	116.8	152.7
X1	122.5	160.1	118.7	155.2
SB	118.5	155.0	115.0	150.4
SU1	133.6	174.7	130.7	170.8
SU2	110.7	144.8	106.4	139.1
F1	100.8	131.8	98.4	128.6
F2	123.1	160.9	119.7	156.4

Table 4 presents the measured prestress losses; both initial and time-dependent losses were calculated as a percentage of the jacking prestress (measured as described above).

Table 4 – Measured prestress losses

Specimen	Initial losses (%)	Concrete age at release (days)	Long-term losses (%)	Total prestress loss (%)	Concrete age at load test (days)
SC	1.7	4	4.7	6.4	288
XC	1.9	4	3.7	5.6	155
FC	1.7	4	6.4	8.2	314
X1	1.4	7	3.0	4.4	29
SB	3.7	6	2.8	6.6	23
SU1	1.4	6	2.2	3.6	16
SU2	1.8	12	3.8	5.7	23
F1	4.7	7	2.3	6.9	22
F2	2.0	7	2.7	4.7	45

The measured prestress losses compare well with typical 25-50 ksi (12-25% of a specimen stressed to $0.75f_{pu}$) of prestress losses (due to all immediate and long-term effects) observed in typical prestressed concrete sections[3]. The measured losses for all specimens were at the lower end of this range.

Predicted prestress losses were also computed for comparison using the PCI method – though the prediction methods are intended only for pretensioned girders consisting of normal weight concrete and 270 ksi prestressing strand[11]. Though the spliced specimens do not fall into this category, the estimates were calculated and are provided for general reference. The specified concrete strength at transfer and the specified 28-day strength was

used to estimate the modulus of elasticity at transfer as 4,630 ksi and at time of loading as 5,500 ksi (per ACI, $E = 33{,}000 w_c^{1.5} \sqrt{f'_c}$). Relative humidity was assumed to be 75%. Figure 19 compares the measured and PCI predicted losses. In all cases, the PCI predicted prestress loss is greater than the measured loss. Overestimation of prestress losses by PCI has been observed by other researchers[12].

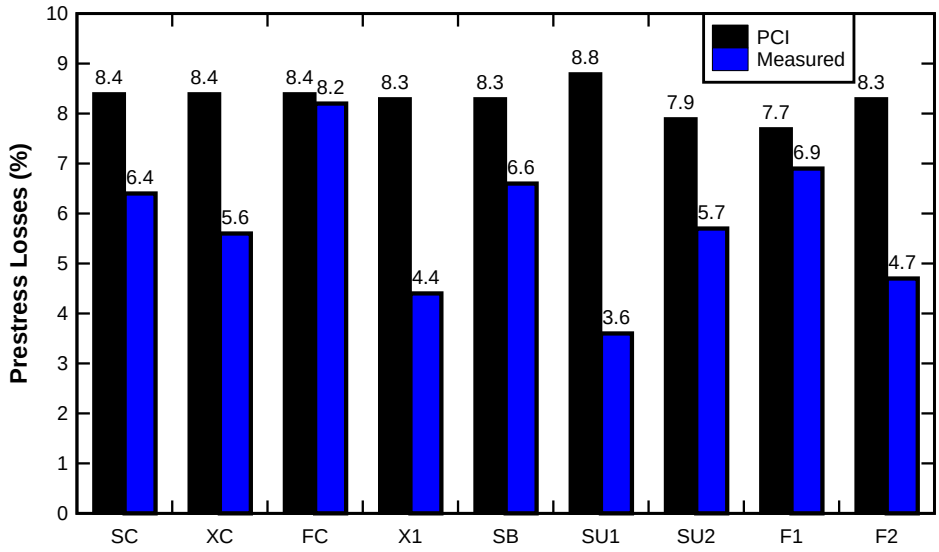

Figure 19–Measured prestress losses vs. PCI

FLEXURAL BEHAVIOR AND COMPARISON TO AASHTO

Two specimens were loaded monotonically in four-point bending to evaluate flexural behavior: one control specimen (XC) and one spliced specimen (X1). This section summarizes the results and compares them to AASHTO code calculated values. Detailed discussion can be found in the FDOT report[10].

In both tests, load was applied at 0.2 kip/sec. When cracking was first visually observed, the load was held. The specimen was inspected, and cracks were marked. Load application was then resumed at 0.2 kip/sec until termination of the load test. The test was terminated when either compressive failure occurred in the deck concrete or when excessive deflection of the specimen threatened the instrumentation. In both tests, the flexural capacity (maximum load) was reached prior to end of test. Strain, strand slip, load, and displacement were monitored throughout the test. The test set-up is shown in Figure 20.

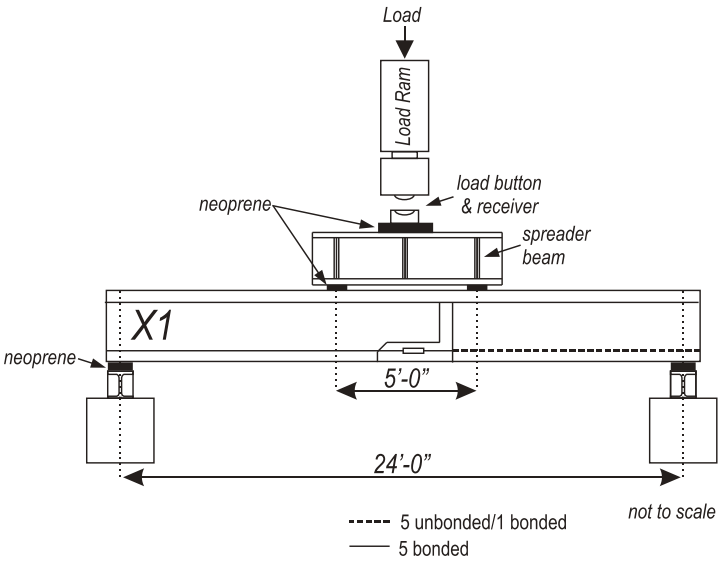

Figure 20–Four-point flexural test set-up showing the splice location

The XC specimen cracked at an applied load of 77 kip, while the spliced X1 specimen developed a joint opening at 64 kip. These applied loads correspond to an approximate bottom fiber stress of $3.8\sqrt{f'_c}$(psi) and $2.2\sqrt{f'_c}$(psi) in XC and X1, respectively. Potential causes for the low cracking load of X1 were investigated, including the low specified jacking prestress of $0.6f_{pu}$ (vs. the more typical $0.75\ f_{pu}$), the achieved initial prestress level at lock-off, and measured prestress losses. No cause was identified. The low "cracking load" of X1 is more understandable; the first crack occurred at the vertical interface of the closure pour. The "cracking load" of X1 was the load required to overcome bond at the dry joint between the precast segment and CIP splice concrete. Consequently, a lower load - slightly greater than that required to reach the decompression moment–is required to open the joint

Beyond cracking, the specimens continued to exhibit disparate behavior. XC continued to develop cracks typically of a continuously bonded prestressed beam: cracks were well-distributed and of small width. In contrast, like in segmental bridge beams with unbonded tendons, the primary crack of X1 formed at the joint. After cracking, this primary crack continued to open with additional applied load, while the adjacent unbonded segment remained uncracked.

Loading of XC was terminated at a deflection of approximately 3.9 in. and a maximum load of 158 kip to avoid damage to instrumentation. Measured compressive concrete strains in the top of the deck at midspan were near 0.003 at termination of the test and the load-deflection plot was nearly flat, indicating that the prestressing strands were yielding and that the specimen's actual flexural strength would not have been significantly higher.

X1 reached peak load at 144 kip and a midspan deflection of 2.6 in. Following a load drop of approximately 2 kip, the specimen continued to deflect without resisting additional load. Failure of X1 occurred when the deck above vertical interface crushed; the failure was accompanied by pronounced vertical deflection of the specimen prior to deck failure.

Figure 21 shows the load-deflection plots for both specimens XC and X1. Also shown is the AASHTO computed flexural strength – assuming unbonded or bonded strand. The strength was computed in accordance with AASHTO-LRFD using specified material strengths of 4.5 ksi deck concrete and 270 ksi prestressing steel. The predicted bonded moment capacity at 0.003 concrete compressive strain was 631 kip-ft. For both XC and X1, the peak load exceeded the predicted design strength of a bonded prestressed member. Considering the unbonded strand in the spliced region of the X1specimen, the AASHTO-LRFD capacity was also calculated assuming the steel strands were unbonded. The calculated moment strength, assuming all five strands were unbonded, was 589 kip-ft. X1 exceeded the anticipated capacity of an unbonded section.

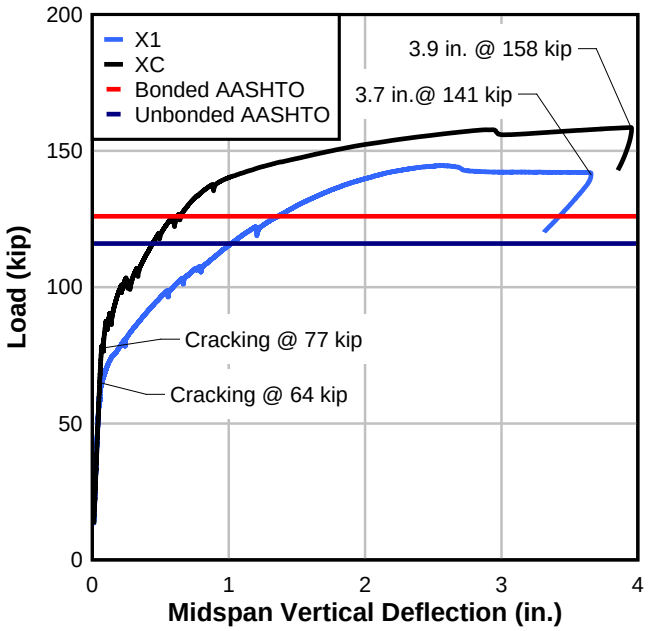

Figure 21–Load-deflection: XC and X1

SUMMARY AND CONCLUSIONS

A new splice technique was developed to lengthen the span of transportable precast prestressed concrete girders. The splice design focused on an intended application: a simply-supported I-girder with a span length of greater than 200 ft. Utilizing the FDOT's longest spanning I-girder section, the FIB96, a prototype beam design for a 208-ft simply-supported span provided the shear and moment demand on the splice for an example case. The bridge was designed in accordance with AASHTO-LRFD 2007 and the FDOT Structural Design Guidelines [8,9].

A splice design was then developed and integrated into the prototype design. The splice design assembly procedures and prestress losses were evaluated using nine AASHTO Type II specimens; three control specimens and six spliced specimens were fabricated. To accomplish this, fifteen precast prestressed segments were constructed at a precast facility. The precast segments were then transported to the FDOT Structures Research Lab where six

spliced specimens were assembled, splices stressed and closures poured. The assembly and stressing procedure included instrumentation to evaluate the procedure. Prestress losses were measured and cracking development was observed to assess service behavior. Flexure, shear, and fatigue tests were conducted with the result of the flexural tests reported herein. Significant findings include:

- Observed prestress losses in the splice region ranged from 5 to 10%, which is less than typical values (10-20%).
- Crack opening occurred primarily at the vertical interface of the closure pour in flexural tests of the spliced specimens.
- Flexural strength of spliced specimens exceeded the AASHTO-LRFD values for bonded strand by 15% and for unbonded strand by 24% when using specified material strengths to compute strength.
- Though labor-intensive, the prestressed splice concept was constructible.

REFERENCES

1. Abdel-Karim, A. M., and Tadros, M. K. (1992). "State-of-the-Art of Precast/Prestressed Concrete Spliced I-Girder Bridges" Precast/Prestressed Concrete Institute, Chicago, IL.
2. Castrodale, R. W., and White, C. D. (2004). *NCHRP Report 517: Extending Span Ranges of Precast Prestressed Concrete Girders*. (Vol. 517). Transportation Research Board, Washington D.C.
3. PCI. (2004). *PCI Design Handbook: 6th Edition*, Precast/Prestressed Concrete Institute, Chicago, IL.
4. Wiegel, J. A., Seguirant, S.J., Brice, R. and Khaleghi, B. (2003) "High Performance Precast, Pretensioned Concrete Girder Bridges in Washington State." PCI Journal, 48(2), 28-52.
5. Abdel-Karim, A. M., and M. K. Tadros. (1992). "Design and Construction of Spliced I-Girder Bridges." *PCI Journal*, 37(4), 114-122.
6. Nicholls, J. J., and Prussack, C. (1997). "Innovative Design and Erection Methods Solve Construction of Rock Cut Bridge." PCI Journal, 42(4), 42-55.
7. Gerwick, B. C., Jr. (1993). *Construction of Prestressed Concrete Structures.* 2nd Ed. Wiley-Interscience, New York, NY.
8. AASHTO. (2007). *AASHTO LRFD Bridge Design Specifications (4th edition with 2007 interim revisions).* American Association of State Highway and Transportation Officials, Washington D.C.
9. FDOT (Florida Department of Transportation). (2010). FDOT *Structures Manual*, FDOT, Tallahassee, FL.
10. Brenkus, N.R. and Hamilton, H.R. (2013). "Long Spans with Transportable Precast Prestressed Girders." FDOT Research Report No. BDK75 977-30, Florida Department of Transportation, Tallahassee, FL.
11. Zia, P. and Mostafa, T. (1977). "Development Length of Prestressing Strands." *PCI Journal*, 22(5), 54-65.

12. Onyemelukwe, O.U., Moussa Issa, P.E., and Mills, C.J. (2003). "Field Measured Prestress Concrete Losses Versus Design Code Estimates." Experimental Mechanics. 43(2), 201-215.